Available online at www.sciencedirect.com
ScienceDirect
Ceramics International 36 (2010) 827–829
CERAMICS INTERNATIONAL
www.elsevier.com/locate/ceramint

Short communication

Thermo-analysis of nanocrystalline TiO_2 ceramics during the whole sintering process using differential scanning calorimetry

Da Li [a,b,*], Shaou Chen [c,d,**], Dechang Wang [a], Yanhui Li [a,d], Weiquan Shao [c], Yunze Long [b,c], Zongwen Liu [b], Simon P. Ringer [b]

[a] College of Mechanical Engineering, Qingdao University, Qingdao 266071, PR China
[b] Australian Key Centre for Microscopy and Microanalysis, The University of Sydney, NSW 2006, Australia
[c] College of Physics Science, Qingdao University, Qingdao 266071, PR China
[d] Laboratory of Fiber Materials and Modern Textile, the Growing Base for State Key Laboratory, Qingdao University, Qingdao 266071, PR China

Received 9 April 2009; received in revised form 15 May 2009; accepted 2 October 2009
Available online 4 November 2009

Abstract

The thermodynamics of nanocrystalline TiO_2 ceramics during the whole sintering process were analyzed using differential scanning calorimetry (DSC) for different heating rates (10, 20 and 30 °C/min). The raw TiO_2 powder was also studied comparably. The DSC and specific heat capacity (C_p) were also studied. The results show that there is no obvious endothermic or exothermic peak at the stage where the maximum densification rate occurred for TiO_2 ceramics. The ordering process induced by the microstructural densification counteracts the disordering process induced by increasing the sintering temperature. The sintering process is a result of combination of the ordering process and the disordering one. The activation energy of nanometer TiO_2 ceramics determined by Kissinger method is 103.8 kJ/mol.

Keywords: A. Sintering; D. TiO_2; Ceramics; Differential scanning calorimetry (DSC); Thermodynamics

1. Introduction

Nanocrystalline TiO_2 powder is widely used for its catalytic, photo-catalytic and gas-sensing properties. Moreover, nanocrystalline TiO_2 ceramics are also of great importance due to the low-creep and superplastic property at room temperature [1–3]. To fabricate titania ceramics with controlled density and grain size, it is necessary to carry out a thorough analysis of sintering.

Since the 1940s, many sintering theories have been proposed and verified by experiments. Much attention was paid to the sintering mechanism and microstructural evolution. The relative density and the grain size were usually investigated as functions of sintering time, sintering temperature, heating rate, and green relative density [4–8].

To our knowledge, little attention has been given to the thermodynamics of TiO_2 during the whole sintering process. It has been found that there exists a maximum densification rate for TiO_2 ceramics during the sintering [9]. To understand the sintering kinetics controlling grain growth and densification, it is important to determine the activation energy for the diffusion mechanisms and analyze the thermal behavior during the whole sintering process. The aim of the present research is to investigate the DSC and C_p behavior of TiO_2 ceramics during the whole sintering, especially at the temperature where a maximum densification rate occurred. The sintering kinetics of raw TiO_2 powders was also investigated comparably.

The activation energy has been determined by various methods, such as isothermal and non-isothermal sintering [10–12]. The isothermal analysis is more unambiguous but the experiments are generally very time-consuming, thus the non-isothermal experiments (experiments performed at constant heating rate) seem to be more favorable. These types of experiment are attractive for their rapidity and also for the

* Corresponding author at: College of Mechanical Engineering, Qingdao University, Qingdao 266071, PR China. Tel.: +86 532 85952321; fax: +86 532 85955977.
** Corresponding author at: College of Physics Science, Qingdao University, Qingdao 266071, PR China. Tel.: +86 532 85952321; fax: +86 532 85955977.
E-mail address: lida889@126.com (D. Li).

0272-8842/$36.00
doi:10.1016/j.ceramint.2009.10.004

extension of the temperature range of measurement. In the industry processes, the systems often undergo phase transformation under non-isothermal conditions. For these reasons, the non-isothermal experiments are preferably used in the study of the thermal behaviors during sintering.

Currently, the apparent activation energy is often determined under linear heating conditions using the equation derived by Kissinger [13–15]:

$$\ln\frac{T^2}{\alpha} = \frac{E}{kT} + C \quad (1)$$

where k is the Boltzmann's constant, α is the heating rate, E is activation energy, C is a constant and T is absolute temperature which is dependent on the heating rate.

The heating rate (α) and the peak temperature T_P conform to the following equation:

$$\frac{d[\ln(\alpha/T_P^2)]}{d(1/T_P)} = -\frac{E}{R} \quad (2)$$

where R is gas constant. Then, the activation energies (E) can be determined from a plot of $\ln(\alpha/T_P^2)$ versus $1/T_P$.

2. Experimental procedure

The raw materials used in the experiment were 99.9% rutile TiO_2 (Zhoushan Nanomaterials Co., China) with a mean particle size of 50 nm. The as-received powder was first pressed in a mold at room temperature at 40 MPa. Then, the green sample was pressed by cold isostatic pressing at 200 MPa with a dwell time of 10 min. The sample was milled to small pellets with a size of 78–156 μm. The pellets were used the DSC testing and the as-received TiO_2 powder was used as reference sample.

The DSC was performed with a NETZSCH DSC 404 (NETZSCH Co., Germany). About 10 mg sample was used for DSC testing and α-Al_2O_3 powder as the reference sample. The heating temperature range was from room temperature to 1300 °C at heating rates of 10, 20 and 30 °C/min. The measurement was carried out in nitrogen flow at the rate of 20 ml/min.

3. Results and discussion

Fig. 1 shows the non-isothermal DSC curves of the raw TiO_2 powder at the heating rates of 10, 20, and 30 °C/min. There is a small endothermic peak at 140–150 °C in each curve, which corresponds to the volatilization of water and organic material. At a higher temperature range of 400–900 °C, a strong exothermic peak was observed which was induced by the crystallization process of amorphous TiO_2 to crystalline TiO_2. It shows that there is a small quantity of amorphous TiO_2 in raw materials. With the increasing heating rate, the exothermic peak shifted to higher temperature and the peak became stronger. At a higher heating rate (30 °C/min), the amorphous TiO_2 transformed to rutile directly while at a lower heating rate

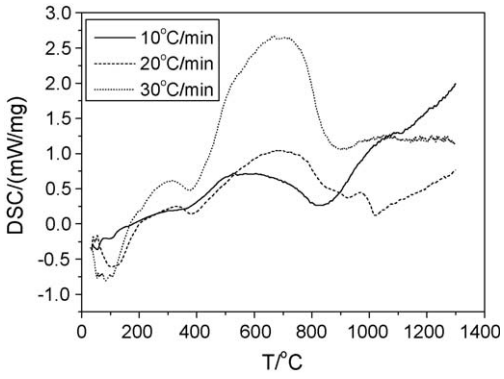

Fig. 1. DSC curves of raw TiO_2 powder at heating rates of 10, 20, and 30 °C/min.

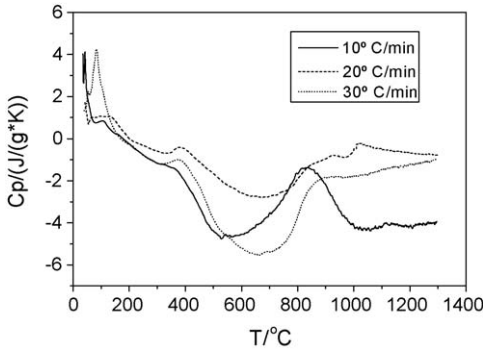

Fig. 2. Specific heat capacity curves of raw TiO_2 powder at heating rates of 10, 20, and 30 °C/min.

(10 °C/min), the amorphous transformed to anatase at 500 °C, then to rutile at 800–900 °C.

To illustrate the heat behavior during sintering, the specific heat capacity (C_p) of raw TiO_2 powder was measured. Fig. 2 shows variations of the specific heat capacity (C_p) with temperature at different heating rates. At higher heating rates (20, 30 °C/min), there exists an endothermic peak at a temperature range of 400–900 °C. However, when the heating rate is low (10 °C/min), there are an endothermic and an exothermic peak, which correspond to the crystallization peak and phase transformation from anatase to rutile respectively. The C_p curves are consistent with the DSC curves. The specific heat capacity is nearly a constant when the temperature reached to 900–1000 °C. With the increasing temperature, the value of C_p increases slightly, which indicates that the heat behavior is very stable.

The peak temperature T_P at which phase transformation peak appeared at different heating rates is listed in Table 1. Then, the activation energies (E) can be determined from a plot of $\ln(\alpha/T_P^2)$ versus $1/T_P$. The slop of $\ln(\alpha/T_P^2)$ versus $1/T_P$ is -12.4809×10^3 and the derived activation energy is 103.8 kJ/mol.

Fig. 3 shows the DSC curves of TiO_2 ceramic at the heating rates of 10, 20 and 30 °C/min. There is a sharp endothermic peak at 140–150 °C, which corresponds to the volatilization of water and organic material. The endothermic peak shifted to higher temperature and became sharp with the increasing heating rate. There is no obvious peak at 200–1300 °C. The reason is that the amorphous TiO_2 had crystallized when the

Table 1
The sintering kinetics data by Kissinger method obtained from Fig. 1.

Heating rate, α (°C)	T_P (°C)	T_P (K)	$1/T_P$ ($\times 10^3$ K^{-1})	$\ln(\alpha/T_P^2)$
10	606	879	1.1377	−11.2549
20	659	932	1.0729	−10.6790
30	708	981	1.0194	−10.3759

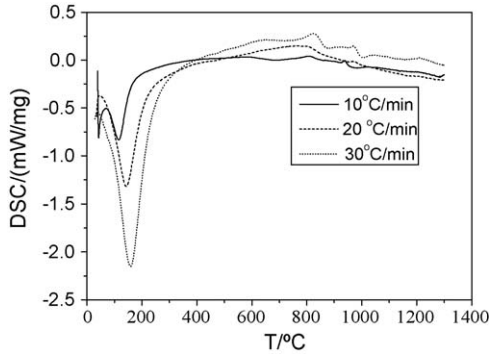

Fig. 3. DSC curves of TiO_2 ceramic at heating rates of 10, 20, and 30 °C/min.

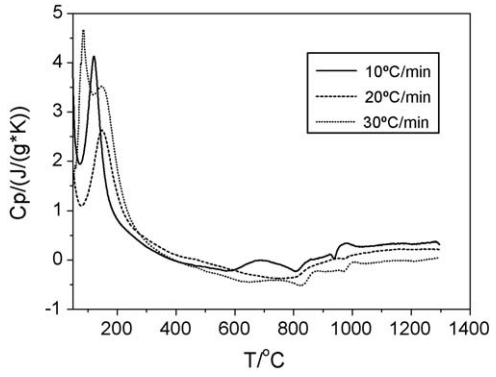

Fig. 4. Specific heat capacity curves of TiO_2 ceramic at heating rates of 10, 20, and 30 °C/min.

binder was removed at 500 °C. So there is no phase transformation occurred during 400–900 °C.

Fig. 4 shows the specific heat capacity (C_p) of TiO_2 ceramic at different heating rates. It can be seen that the C_p is nearly a constant at a temperature range of 600–1300 °C and it increases slightly with the increasing of temperature. The results mean that the absorbed heat does not increase sharply at the maximum densification rate. The relationship of specific heat capacity and temperature can be fitted to line equation as $C_p = -0.7 + 8.79 \times 10^{-4}T$ J/(g K), $R = 0.89$. Compared with the specific heat capacity curve of raw powder (in Fig. 2), the pellets have no peak at a range of 400–900 °C. The pellets have finished the crystallization process during the binder removing process. There is no crystallization peak or phase transformation during the subsequent sintering [16–18].

4. Conclusions

In summary, there is no obvious endothermic or exothermic phenomenon where the maximum densification rate occurs during the sintering. The thermal analysis shows that the microstructural ordering process induced by the densification offsets the disordering process induced by increasing the sintering temperature. The sintering process is a result of combination of the ordering process and the disordering one.

Acknowledgement

The financial support from Natural Science Foundation of Shandong Province (Grant No. Y2008F13) and National Natural Science Foundation of China (Grant No. 50806035, 50802045) are gratefully acknowledged.

References

[1] Y.-I. Lee, Y.-W. Kim, M. Mitomo, et al., Fabrication of dense nanostructured silicon carbide ceramics through two-step sintering, J. Am. Ceram. Soc. 86 (2003) 1803–1805.
[2] P. Billik, G. Plesch, Mechanochemical synthesis of nanocrystalline TiO_2 from liquid $TiCl_4$, Scr. Mater. 56 (2007) 979–982.
[3] R. Yuan, X. Fu, P. Liu, X. Wang, Kinetics of initial stage of sintering from shrinkage data, Scr. Mater. 55 (2006) 1003–1006.
[4] J. Frenkel, Viscous flow of crystalline bodies under the action of surface tension, J. Phys. 9 (1945) 385.
[5] W.D. Kingery, M. Berg, Study of initial stages of sintering solids by viscous flow, evaporation–condensation, and self-diffusion, J. Appl. Phys. 26 (1955) 1205–1212.
[6] L.A. Pérez-Maqueda, J.M. Criado, C. Real, Influence of solvents on morphology of TiO_2 fibers prepared by template synthesis, J. Am. Ceram. Soc. 85 (2002) 763–768.
[7] H.T. Wang, X.Q. Liu, Kinetics and mechanism of a sintering process for macroporous alumina ceramics by extrusion, J. Am. Ceram. Soc. 81 (1998) 781–784.
[8] B.-G. Guillaume, G. Christian, Apparent activation energy for the densification of a commercially available granulated zirconia powder, J. Am. Ceram. Soc. 90 (2007) 1246–1250.
[9] D. Li, S. Chen, W. Shao, X. Ge, Densification evolution of TiO_2 ceramics during sintering based on the master sintering curve theory, Mater. Lett. 62 (2008) 849–851.
[10] J. Holubová, Z. Černošek, E. Černošková, Crystallization of supercooled liquid of selenium: the comparison of kinetic analysis of both isothermal and non-isothermal DSC data, Mater. Lett. 60 (2006) 2429–2432.
[11] T. Wanga, A. Dorner-Reiselb, Thermo-analytical investigations of the decomposition of oxyhydroxyapatite, Mater. Lett. 58 (2004) 3025–3028.
[12] V.A. Khonik, K. Kitagawa, H. Morii, On the determination of the crystallization activation energy of metallic glasses, J. Appl. Phys. 87 (2000) 8440–8443.
[13] H.E. Kissinger, The crystallization kinetics with heating rate in differential thermal analysis, J. Res. Natl. Bur. Stand. 57 (1956) 217–221.
[14] H.E. Kissinger, Reaction kinetics in differential thermal analysis, Anal. Chem. 29 (1957) 1702–1706.
[15] R.-H. Fana, B. Liua, J. de Zhanga, et al., Kinetic evaluation of combustion synthesis $3TiO_2 + 7Al \rightarrow 3TiAl + 2Al_2O_3$ using non-isothermal DSC method, Mater. Chem. Phys. 91 (2005) 140–145.
[16] J.M. Sung, S.E. Lin, W.C.J. Wei, Synthesis and reaction kinetics for monodispersive Y_2O_3:Tb^{3+} spherical phosphor particles, J. Eur. Ceram. Soc. 27 (2007) 2605–2611.
[17] C.-S. Hsi, H.-Z. Cheng, H.-J. Hsu, Crystallization kinetics and magnetic properties of iron oxide contained $25Li_2O$–$8MnO_2$–$20CaO$–$2P_2O_5$–$45SiO_2$ glasses, J. Eur. Ceram. Soc. 27 (2007) 3171–3176.
[18] V. Cannillo, F. Pierli, S. Sampath, C. Siligardi, Thermal and physical characterisation of apatite/wollastonite bioactive glass–ceramics, J. Eur. Ceram. Soc. 29 (2009) 611–619.